International Journal of Heat and Mass Transfer 143 (2019) 118600

Contents lists available at ScienceDirect

International Journal of Heat and Mass Transfer

journal homepage: www.elsevier.com/locate/ijhmt

Enhancing opto-thermal performances of the reflective phosphor-converted laser diode by stacking a sapphire substrate for double-sided phosphor cooling

Yupu Ma, Xiaobing Luo *

School of Energy and Power Engineering, Huazhong University of Science and Technology, Wuhan 430074, China

ARTICLE INFO

Article history:
Received 2 July 2019
Received in revised form 19 August 2019
Accepted 19 August 2019

Keywords:
Phosphor heating
Laser diodes
Phosphor temperature
Double-sided cooling
Sapphire

ABSTRACT

Phosphor-converted laser diode (pc-LD) has been a very competitive candidate in high-luminance white illumination. For the reflective pc-LD, the phosphor layer is usually bonded onto a reflective substrate, which plays the role of light reflection and heat dissipation. However, the heat generation of phosphor cannot be efficiently dissipated by only cooling the reflective surface, in which case most of heat may be confined in the phosphor layer with low thermal conductivity. In this work, a double-sided phosphor cooling scheme was presented to improve the opto-thermal performances of the reflective pc-LD by stacking a highly transparent and heat-conducting sapphire substrate onto the phosphor layer. By using an opto-thermal phosphor model, it was found that the maximum heat generation density and hotspot were both confined at the incident surface. After stacking a sapphire substrate onto the incident surface, the maximum heat was extracted and conducted from the sapphire substrate to the reflective substrate, leading to a significant decrease of the maximum phosphor temperature from 221 °C to 86 °C under excitation power of 0.8 W. In this case, a higher excitation power was allowed, contributing to a higher attainable output power and luminance. The double-sided phosphor cooling scheme was also experimentally achieved. It was found that the presented scheme exhibited higher optical power, luminance and color stability than the traditional one under higher excitation power.

1. Introduction

Laser diode (LD) has been considered to be a very promising solid-state light source in the future high-luminance illumination with the advantage of no efficiency drop [1,2] and low etendue due to small divergent angle and small emitting area [3,4]. The most common way of achieving laser-based white light is using a blue InGaN/GaN LD to excite yellow cerium-doped yttrium aluminum garnet (YAG:Ce) phosphor, which is also called phosphor-converted laser diode (pc-LD) [5]. To prevent the thermal damage of the phosphor layer from the very high heat flux density of LD, the remote phosphor configuration is always applied [6]. There has been two packaging methods of the remote pc-LD, namely the transmissive pc-LD [7–9] and the reflective pc-LD [10,11]. For the transmissive pc-LD, the phosphor layer is usually fixed to a holder at its periphery. The light incidents on the middle area and then transmits directly through the layer. For the reflective pc-LD, the phosphor layer is usually boned onto a reflective substrate and the light will be reflected on the reflective surface of the substrate.

Because of the high excitation density from LD, the heat generation density of phosphor may be also high, resulting in a very high local phosphor temperature. This has remained a challenging issue to be tackled in high-power pc-LD [12]. It has been reported in our previous work that the maximum phosphor temperature reached 549 °C when the transmissive phosphor was illuminated by a 0.68 W laser spot with a diameter of 1.0 mm [13]. In this case, a significant deterioration of efficiency, reliability, and lifetime occurred, accompanying with severe phosphor thermal quenching and even silicone carbonization phenomenon. To relieve the thermal quenching effect, researchers have been devoted to developing alternative phosphors with high thermal conductivity and high thermal stability, including the phosphor in glass (PiG) [14], ceramic phosphor [15], and single-crystal phosphor [16]. Despite their excellent performances in reducing the phosphor temperature, the complexity of the synthesis process and the high cost may be not so fascinating. Alternatively, the thermal management of phosphor layer may be a simple and direct solution to this problem. For transmissive pc-LD, Correia et al. [17] recently have

* Corresponding author.
E-mail address: luoxb@hust.edu.cn (X. Luo).

https://doi.org/10.1016/j.ijheatmasstransfer.2019.118600
0017-9310/

developed a beam shaping method by redistributing the radiation pattern of the LD on the periphery of the phosphor layer, where the heat can be effectively dissipated through the holder. In addition, the phosphor temperature can be reduced by increasing the heat dissipation area. Based on this point, one side [18] or double sides [19] of phosphor layer was bonded with a sapphire substrate with high transmission ratio and thermal conductivity ($\sim$30 $W{\cdot}m^{-1}{\cdot}K^{-1}$).

Compared with the transmissive pc-LD, the reflective pc-LD possesses better thermal stability because the heat can be dissipated through the highly-conducting reflective substrate to some extent. For the reflective pc-LD, the thermal designs are conducted on the bottom surface of the reflective substrate, including the heat sink [20], rotating wheel [21], heat pipe [22], and thermoelectric cooler [23]. Chang et al. [21] coat yellow and green phosphor layers onto a reflective aluminum substrate connected with a micromotor, which is termed as rotating wheel. Due to the excellent heat dissipation ability of the rotating part, this scheme exhibits stable output power and chromatic performance even under excitation power of 30 W. Ding et al. [22] reveal that the coating the phosphor layer onto a heat pipe substrate could maintain an obviously lower phosphor temperature compared with the aluminum substrate. And the maximum sustainable driven power of the heat pipe substrate is 34.4 W, which is 14.7% higher than the aluminum substrate. However, considering that the generated heat is distributed throughout the phosphor [24–26], the heat near the incident surface may be easily confined due to the relatively low thermal conductivity of the phosphor layer. In this case, the thermal design cannot reach their full potential, limiting the attainable optical power and luminance.

In this work, aiming at enhancing the opto-thermal performances of the reflective pc-LD, a double-sided phosphor cooling scheme is proposed by stacking a sapphire substrate onto the incident phosphor surface. The addition of the heat conductive path for the heat near the incident surface is expected to further reduce the phosphor temperature, contributing to the improvement of the optical power and luminance under high excitation power. The effects of the sapphire substrate on the opto-thermal performances of the reflective pc-LD are investigated by an opto-thermal phosphor model as well as experiments.

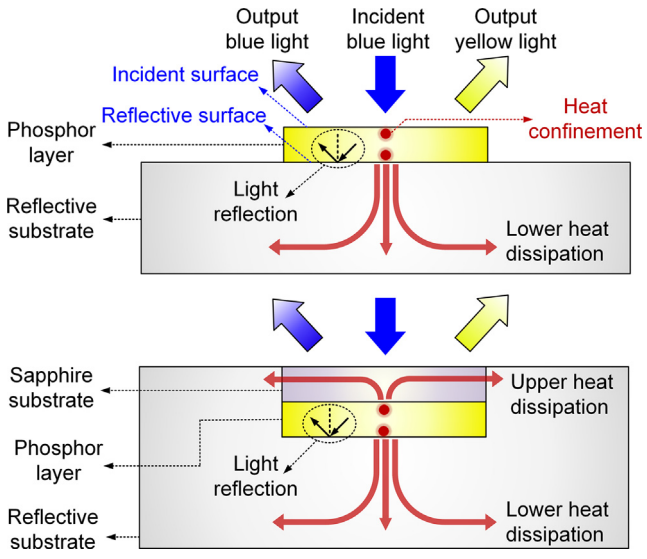

Fig. 1. The schematic and working principle of (a) the traditional reflective pc-LD with one-sided phosphor cooling scheme and (b) the presented reflective pc-LD with double-sided phosphor cooling scheme by stacking a sapphire substrate.

2. Problem statement

Fig. 1(a) shows the schematic and working principle of the traditional pc-LD consisting of a phosphor layer bonded onto a reflective substrate. It should be noted that the upper surface of the reflective substrate is designed to have a high reflectivity. When a blue laser beam emitting from the LD incidents downward onto the phosphor layer, part of blue light is absorbed by the phosphor particles and down-converted into yellow light. Then, the rest of blue light and converted yellow light are reflected on the reflective surface and travel upward into the phosphor layer. In this case, the output blue and yellow lights will transmit from the incident surface and mix with each other, resulting in white light eventually. It should be pointed out that there is also heat generation throughout the phosphor along with the light conversion process, which mainly consists of the Stokes shift loss and quantum efficiency loss [13].The heat near the reflective surface can be easily conducted to the reflective substrate with a high thermal conductivity and dissipated into the environment efficiently. This configuration is also called one-sided phosphor cooling scheme. However, the heat near the incident surface may be confined due to the relatively low thermal conductivity of the phosphor layer, resulting in a high local phosphor temperature or even phosphor thermal quenching. To tackle this problem, besides the lower heat dissipation path, an upper heat dissipation path for the generated heat is further established by stacking a sapphire substrate onto the incident surface, which is shown in Fig. 1(b). This configuration is also called double-sided phosphor cooling scheme. Benefitting from the high thermal conductivity of the sapphire substrate, the heat near the incident surface can also be effectively conducted through the sapphire substrate to the reflective substrate.

3. Methods

3.1. Opto-thermal model

In this section, the overall performances of the reflective pc-LD are studied using an opto-thermal model presented in our recent work [27]. Fig. 2 shows the schematic of the phosphor model. Due to the symmetry, the three-dimensional cylindrical geometry is reduced to a two-dimensional axisymmetric rectangle geometry. The light propagation properties in the phosphor layer including the light absorption, scattering, and fluorescence are described by the fluorescent radiative transfer equations (FRTEs) for the excitation blue light and emission yellow light. When a transmissive phosphor is excited by a collimated laser beam, the radiances of

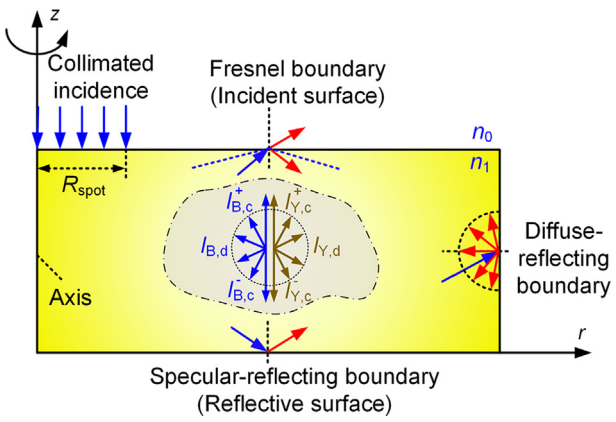

Fig. 2. The two-dimensional axisymmetric phosphor geometry and optical boundary conditions in the opto-thermal model.

the collimated blue $I^{-}_{B,c}$ and yellow lights $I^{-}_{Y,c}$ along the incident direction, diffuse blue $I_{B,d}$and yellow lights $I_{Y,d}$are solved using the discontinuous spectral element method [28]. When it comes to the reflective phosphor, besides the above four light components, the collimated blue$I^{+}_{B,c}$and yellow light$I^{+}_{Y,c}$components along the reflected direction are also introduced due to the light reflection. All the light components are calculated by coding in the commercial software MATLAB. The steps for obtaining these radiances are as follows. First, $I^{-}_{B,c}$ and $I^{+}_{B,c}$ can be obtained based on Beer's law. Next, $I_{B,d}$ along arbitrary diffuse direction is calculated by iteratively solving FRTE for the blue light. The convergence criteria is that the maximum relative error of the radiance between two iterative steps is below 10^{-4}. Then, by inputting all the blue light components as the fluorescent part, the yellow light components, including $I^{-}_{Y,c}$,$I^{+}_{Y,c}$, and $I_{Y,d}$, are solved following the same steps with blue light. The heat generation density in the phosphor can be obtained as the sum of the absorbed radiant fluxes for the blue and yellow lights. By inputting the heat generation density as an internal distributed heat source, the thermal transport property can be described by the heat diffusion equation (HDE), which is solved by the finite element method using the commercial software COMSOL. The FRTEs and HDE are iteratively solved by introducing the temperature-dependent quantum efficiency, in which case the phosphor thermal quenching effect can be further evaluated. The convergence criteria of the opto-thermal interaction is that relative error of the phosphor temperature is lower than 0.01 °C or the minimum quantum efficiency is lower than 0.5 [27]. In this work, we mainly focus on the heat generation density and phosphor temperature.

The optical boundary conditions of the reflective pc-LD are also illustrated in Fig. 2. The LD is modeled as a collimated incident boundary with a Gaussian irradiance distribution on the incident surface. The radius of the laser spot is set to be 1.0 mm. The reflective surface is modeled as a specular-reflecting boundary with a high reflectivity of 0.95. The incident surface is considered as a Fresnel boundary caused by the refractive index mismatch of the phosphor layer and air. It should be noted that the incident surface roughness may pose an effect on the light scattering and transmission, and thus the absorbed radiant fluxes and thermal performances. But this effect is ignored in our model for simplicity. In the future work, this effect can be incorporated into the model by defining the angular reflected and transmitted radiance if a BRDF/BSDF data of the actual surface is provided. The right surface is treated as a diffuse-reflecting boundary with a reflectivity of 0.8. This boundary may have a little effect on the performances considering the large ratio of the phosphor diameter to the laser spot diameter. The left surface is treated as an axis boundary. More details about these boundaries can be found in our previous work [27]. It should be pointed out that the sapphire substrate is assumed to be a transparent medium for simplicity considering the very high transmission ratio in the visible wavelength region. In other words, it is assumed that the sapphire substrate may not affect the optical performance and heat generation density distribution.

As for the thermal boundary conditions, the phosphor layer, sapphire substrate, and reflective substrate are all modeled. The phosphor layer is modeled as a distributed internal heat source as stated above. The bottom surface of the reflective substrate is set to be a Dirichlet boundary with a fixed temperature of 20 °C. All the outer surfaces are set to be Robin boundaries with a natural convective coefficient of 5 $W{\cdot}m^{-2}{\cdot}K^{-1}$, which is calculated using the empirical equation following the previous study [27].

Before conducting the opto-thermal model, some input parameters need to be obtained. The absorption and scattering coefficients of the blue and yellow lights are calculated using the Mie theory [29]. The temperature-dependent quantum efficiency of YAG:Ce phosphor is referred to the reported work [30]. The Henyey-Greenstein (HG) phase function with the anisotropy parameter of 0.82 is used [27]. The phosphor layer is a mixture of phosphor particles and silicone matrix. The refractive indexes of the phosphor layer and sapphire substrate are 1.53 and 1.76, respectively [2]. The thermal conductivities of the phosphor layer, sapphire substrate, and reflective substrate are 0.18 $W{\cdot}m^{-1}{\cdot}K^{-1}$, 30 $W{\cdot}m^{-1}{\cdot}K^{-1}$, and 160 $W{\cdot}m^{-1}{\cdot}K^{-1}$, respectively.

3.2. Experiments

In this section, both the traditional and presented reflective pc-LD are fabricated and tested. The reflective pc-LD consists of LD module and phosphor module. Fig. 3(a) shows the schematic of the process of fabricating the presented reflective phosphor module. The phosphor particles (YAG-04, Intematix) are mixed with the silicone matrix (OE-6550, Dow Corning) to form the phosphor/silicone gel with a phosphor concentration of 0.15 g/cm^3 after vacuuming. Then, the gel is coated onto the reflective surface of the reflective substrate using a volume control method [31]. Next, a commercial cylindrical sapphire substrate (Crystal-Optech) with double-sided anti-reflective coating is stacked onto the phosphor. Finally, the thermal curing process is conducted by placing the whole module on an oven with a fixed temperature of 150 °C for 30 min. The photographs of the reflective substrate and as-fabricated presented phosphor module are shown in Fig. 3(b) and 3(c), respectively. The reflective surface of the reflective substrate is treated using the vacuum plating process to ensure a high reflectivity. The reflective substrate is made of aluminum alloy 6061. Table 1 shows the thermal-physical properties and geometric dimensions of the involving components. The diameters of the phosphor layer and sapphire substrate are both 10 mm, which is same as the inner diameter of the reflective substrate. The thicknesses of the phosphor layer and sapphire substrate are 0.5 mm and 0.3 mm, respectively. The sum of the thickness of the phosphor layer and sapphire substrate is designed to be equal to depth of the hole of the reflective substrate. In addition, the sapphire substrate with a relative small thickness is chosen to avoid light absorption loss. The traditional phosphor module is also fabricated by simply coated the fabricated phosphor layer onto the reflective substrate. To make a fair comparison, the concentration and thickness of the traditional module are consistent with that of the presented module.

Fig. 4 shows the schematic of the experimental setup. The fabricated phosphor module is excited by a commercial laser diode (L450P1600MM, Thorlabs) combined with a collimating lens. Both the LD and lens are mounted in a homemade heat sink to ensure a stable output power. The phosphor module is also mounted on a heat sink via thermal grease. For the optical test shown in Fig. 4 (a), the whole pc-LD is placed inside an integrating sphere (ATA-1000, Everfine) and the output optical power and average correlated color temperature (CCT) are measured. For the thermal test shown in Fig. 4(b), the collimated laser beam incidents onto the phosphor in a small angle of 10° and an infrared (IR) thermal imager (SC620, FLIR) is placed perpendicular to the incident surface, in which case the surface temperature distribution of either the phosphor layer or the sapphire substrate is measured for the traditional or presented reflective pc-LD, respectively. In addition, the luminance of the central spot is measured using the same setup by replacing the IR imager with a spectral radiance colorimeter (SRC-200 M, Everfine). During both optical and thermal tests, varying driving currents from 0 to 1.45 A with an interval of 0.05 A are applied. In each current experiment, the data is recorded until the steady state is reached.

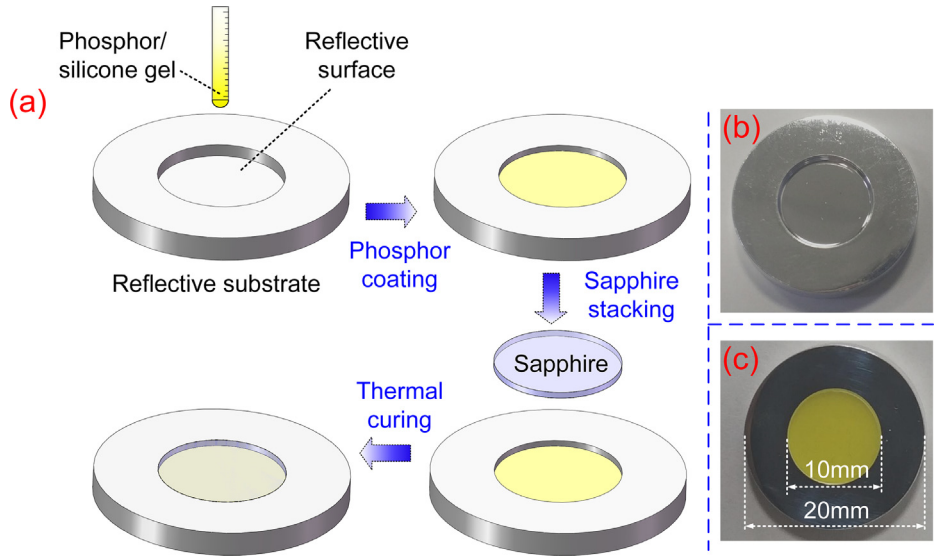

Fig. 3. (a) The process of fabricating the presented reflective phosphor module and the photographs of (b) the reflective substrate and (c) as-fabricated presented phosphor module.

Table 1
The thermal-physical properties and geometric dimensions of the involving components.

Components	Thermal conductivity ($W \cdot m^{-1} \cdot K^{-1}$)	Density ($kg \cdot m^{-3}$)	Heat capacity ($J \cdot kg^{-1} \cdot K^{-1}$)	Diameter (mm)	Thickness (mm)
Phosphor layer	0.18	1140	1300	10	0.5
Sapphire substrate	30	3970	750	10	0.3
Reflective substrate	160	2750	1100	Inner: 10 Outer: 20	/

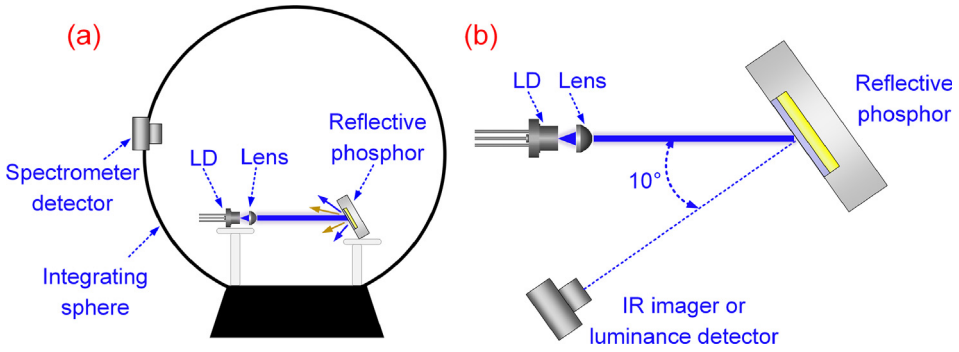

Fig. 4. The schematic of experimental setup of the (b) optical test and (c) thermal test.

4. Results and discussion

4.1. Opto-thermal model

Fig. 5 shows the calculated heat generation density distribution of the phosphor layer under excitation power of 0.8 W. It can be seen that the density increases from the reflective surface to the incident surface along the axis direction. Also, the density reduces from the left surface to the right surface due to the Gaussian incidence. In other words, the maximum density (1.09 W/mm^3) is confined at the center of the incident surface, which is about 1.4 times higher than that at center of the reflective surface (0.45 W/mm^3). This implies that the heat dissipation efficiency of the traditional pc-LD may be not so good by only conducting the minimum heat at the reflective surface. The maximum heat needs additional thermal management to ensure higher thermal performance. It should be noted that there is also a marginal effect of the properties of the sapphire substrate, i.e. the transmission ratio and thickness, on the heat generation density. The sapphire substrate affects the heat generation through the transmitted optical power from the sapphire substrate to the phosphor layer, and the heat generation is proportional to the transmitted optical power. It is obvious that transmitted optical power and heat generation are both proportional to the transmission ratio. As for the thickness of the sapphire substrate, both the transmitted optical power and heat generation decrease exponentially with the thickness under a constant absorption coefficient according to the Beer's law. For low transmission ratio or high thickness case, these need to be considered in the model. Fig. 6 shows the comparisons between the calculated two-dimensional temperature distribution and heat flow of the (a) traditional and (b) presented phosphor module under excitation power of 0.8 W. It can be seen that for the traditional case, there is only one lower heat path to the reflective substrate and the maximum temperature (hotspot) is confined at the center of the

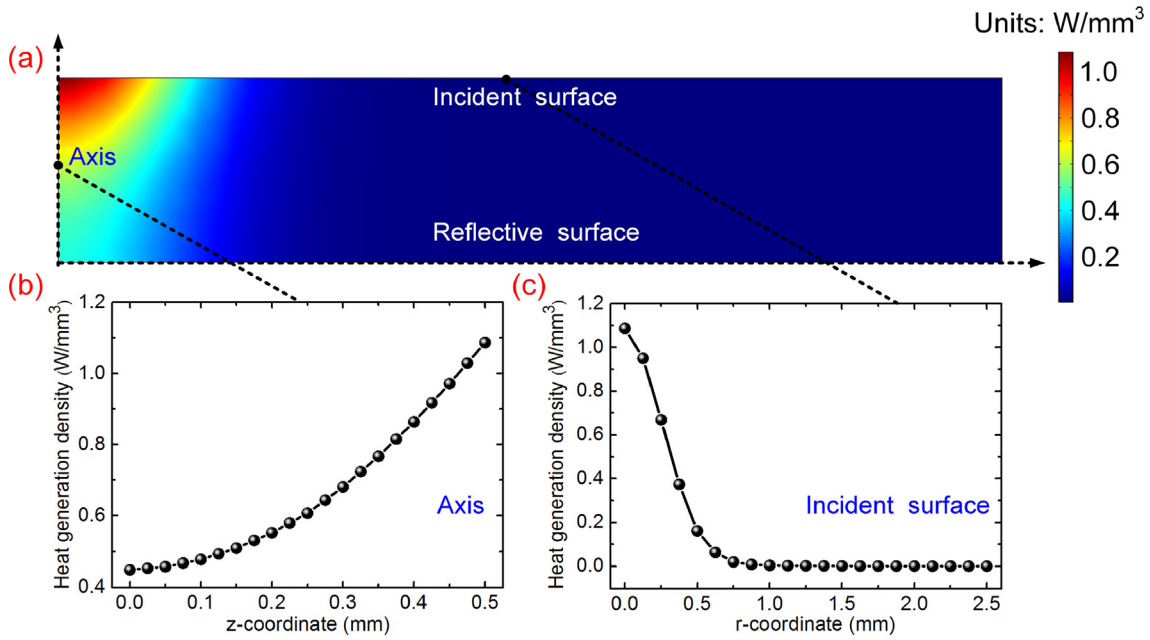

Fig. 5. The calculated (a) two-dimensional heat generation density distribution and cross-sectional distribution of the (b) axis and (c) incident surface under excitation power of 0.8 W.

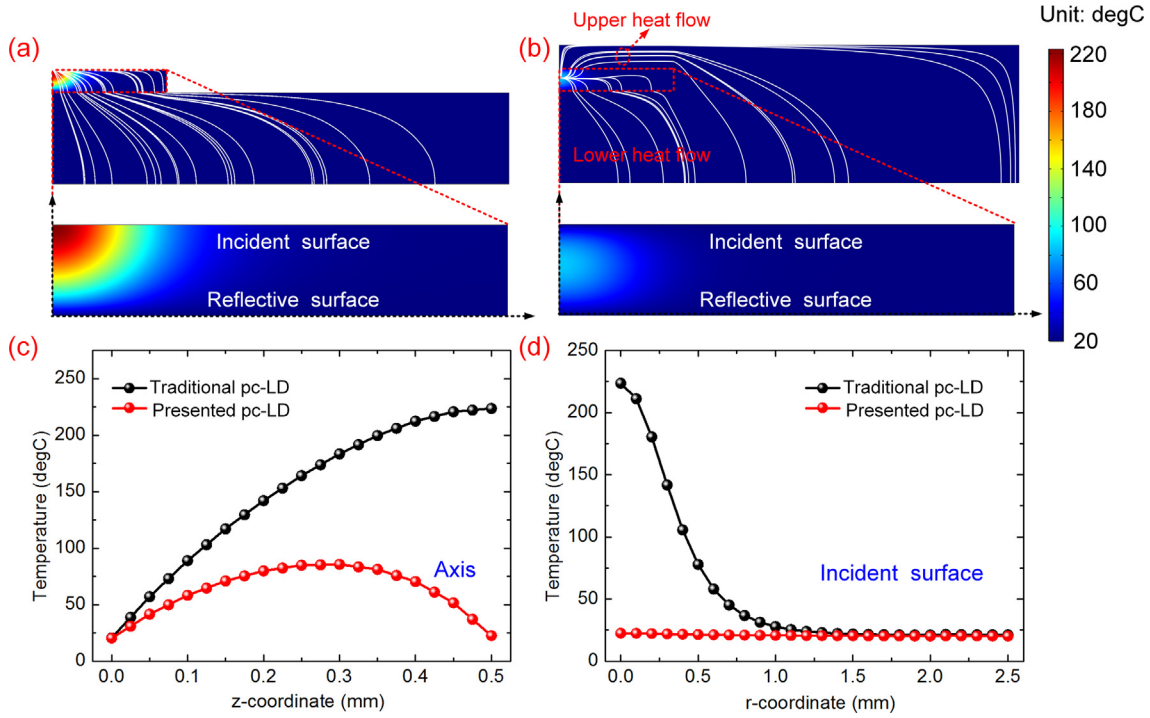

Fig. 6. The calculated two-dimensional temperature distribution and heat flow of the (a) traditional and (b) presented phosphor module; the enlarged figure shows the corresponding temperature distribution of the phosphor layer. The cross-sectional phosphor temperature distribution of the (c) axis and (d) incident surface. All the results are obtained under excitation power of 0.8 W.

incident surface due to the poor natural convection. In contrast, for the presented case, there is another upper heat path from the sapphire substrate to the reflective substrate. In this case, the hotspot shifts from the incident surface to the internal layer on the axis. This is clearly shown in Fig. 6(c). The phosphor temperature of the axis of the traditional case exhibits a constant increase from the reflective surface to the incident surface, whereas that of presented case shows a first increase and then a decrease. In addition, the hotspot of the presented case (86 °C) is 138 °C lower than that of the traditional case (224 °C). As for the temperature distribution on the incident surface shown in Fig. 6 (d), the temperature difference at the central area is very large and the temperature of the presented case remains almost unchanged at a very low value (22 °C). This indicates that the heat generated on the incident surface is effectively dissipated through the sapphire substrate.

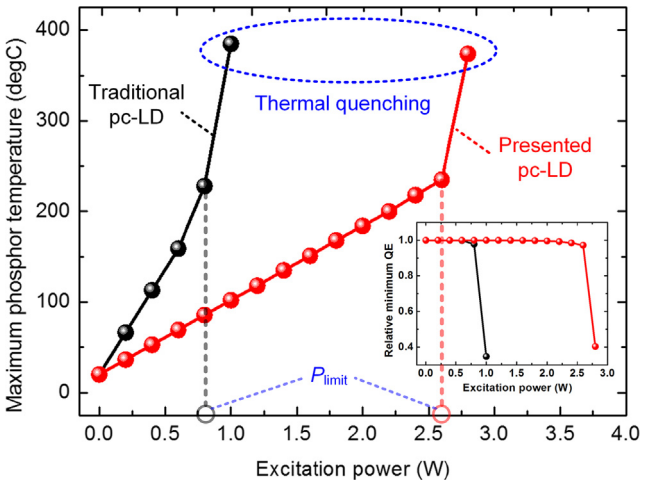

Fig. 7. Comparison of the calculated maximum phosphor temperature between the traditional and presented pc-LD versus varying excitation powers. The inset shows the corresponding relative minimum quantum efficiency.

Fig. 7 shows the comparisons of the maximum phosphor temperature of the traditional and presented pc-LD under varying excitation powers. For both types, the maximum temperature exhibits an approximately linear increase at low excitation power due to the linear rise of power. It can be seen that the rising rate of the traditional type is obviously higher than that of the presented type because of the higher heat dissipation efficiency of the presented type. As the power keeps increasing, the maximum temperature shows a sharp increase and may reach a very high value (>350 °C). In this case, for typical YAG:Ce phosphor, the minimum efficiency corresponding to the maximum temperature reduces sharply to a very low value (<0.4), as shown in the inset figure. This indicates the occurrence of the phosphor thermal quenching. We define the limiting excitation power P_{limit} corresponding to the critical point where the thermal quenching is not occurred, as shown in Fig. 7. Fig. 8 shows the comparison of P_{limit} at varying phosphor concentrations and spot radii. It can be seen that P_{limit} reduces with the increase of the concentration due to the increased absorbed radiant flux. As the spot rises, the excitation power density and heat generation density reduce sharply, resulting in a decrease of P_{limit}. At the same concentration and radius, P_{limit} of the presented type is higher than traditional type, and the difference increases at low concentration and large radius. For example, P_{limit} for traditional type increases from 5.7 W to 15.1 W for the presented type under concentration of 0.05 g/cm^3 and spot radius of 2.5 mm, corresponding to an enhancement of 165%. Therefore, the presented pc-LD can withstand higher excitation power, contributing to the enhancement of the attainable output power and luminance.

4.2. Experimental proof-of-concept

In this section, the experimental proof-of-concept of the presented double-sided phosphor cooling scheme was conducted. Fig. 9(a) and 9(b) show the measured surface temperature distribution of the traditional and presented pc-LD, respectively. There is an obvious hotspot at the center of the phosphor layer for the traditional type, whereas there is an approximately uniform temperature distribution for the presented type. This is clearly illustrated in Fig. 9(c) showing the cross-sectional radial temperature distribution. The reason behind this phenomenon is that the surface temperature of the sapphire substrate rather than the phosphor layer is measured in the presented type. Fig. 9(d) shows the measured maximum surface temperature versus varying driving current. The maximum temperature of the traditional type exhibits the similar trend with model shown in Fig. 7, whereas that of the presented type keeps almost unchanged at a low value, which is also consistent with the finding shown in Fig. 6(d). Considering the phosphor temperature probing of the presented type is restricted in the experiment, the design concept is verified through the optical performances.

Fig. 10(a) shows the emitted power and voltage of LD versus driving currents (P-V-I curves). There is almost no emitted power until the current exceeds 0.15 A, which is the threshold current of LD. As the current increases, the power rise linearly. It should be noted when the current exceeds 1.35 A, the rising rate starts to reduce because of the limitation of thermal management of LD. In this case, the current is only increased to 1.45 A because of the maximum allowable operating current of LD. Fig. 10(b) and 10(c) show the relative spectral power distribution of the traditional and presented pc-LDs, respectively. For the traditional type, when the current rises from 0.25 A to 0.85 A, the spectrum only shows a slight change, but there is a sudden decrease of the yellow spectrum at 0.95 A. In contrast, for the presented type, the yellow spectrum exhibits a slight increase when the current rises from 0.25 A to 1.45 A. The corresponding output power and the average CCT are plotted in Fig. 10(d) and 10(e). The output power of presented type is slightly lower than that of traditional type because of the slight light absorption of the sapphire substrate. When the current is above 0.95 A, the output power of the presented type is much higher than the traditional type because thermal quenching occurs in the traditional type. The same phenomenon is also found for the luminance shown in Fig. 10(f). As for the average CCT, there is also a sudden increase from 5187 K to 10002 K when

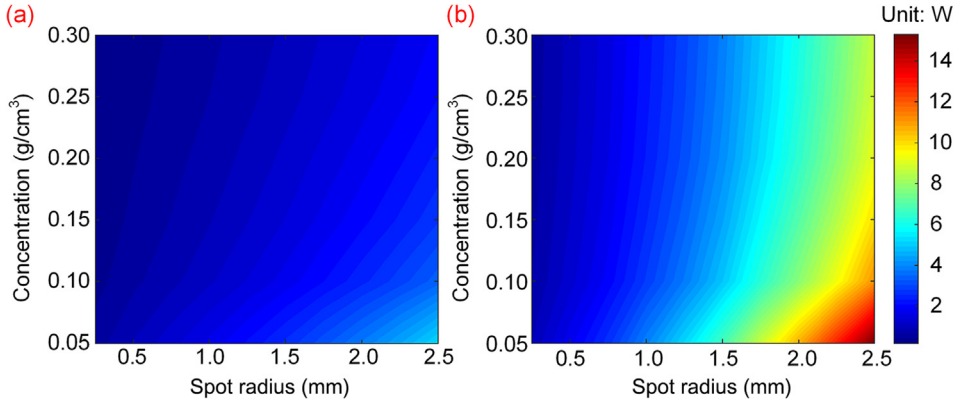

Fig. 8. The limiting excitation power versus varying phosphor concentrations and spot radii of the (a) traditional and (b) presented pc-LD.

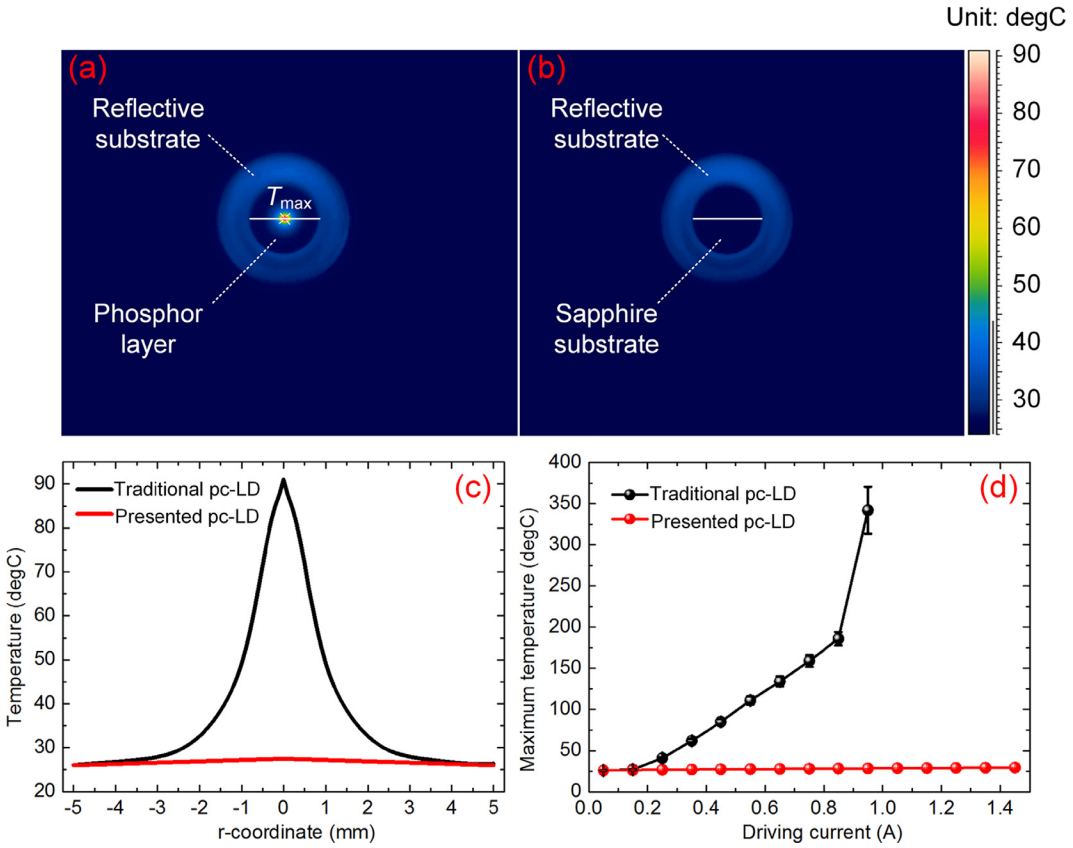

Fig. 9. The measured surface temperature distribution of (a) the traditional and (b) presented reflective pc-LD under driving current of 0.5 A; (c) the corresponding cross-sectional radial temperature distribution of the lines. (d) The comparison of the measured maximum temperature versus varying driving currents.

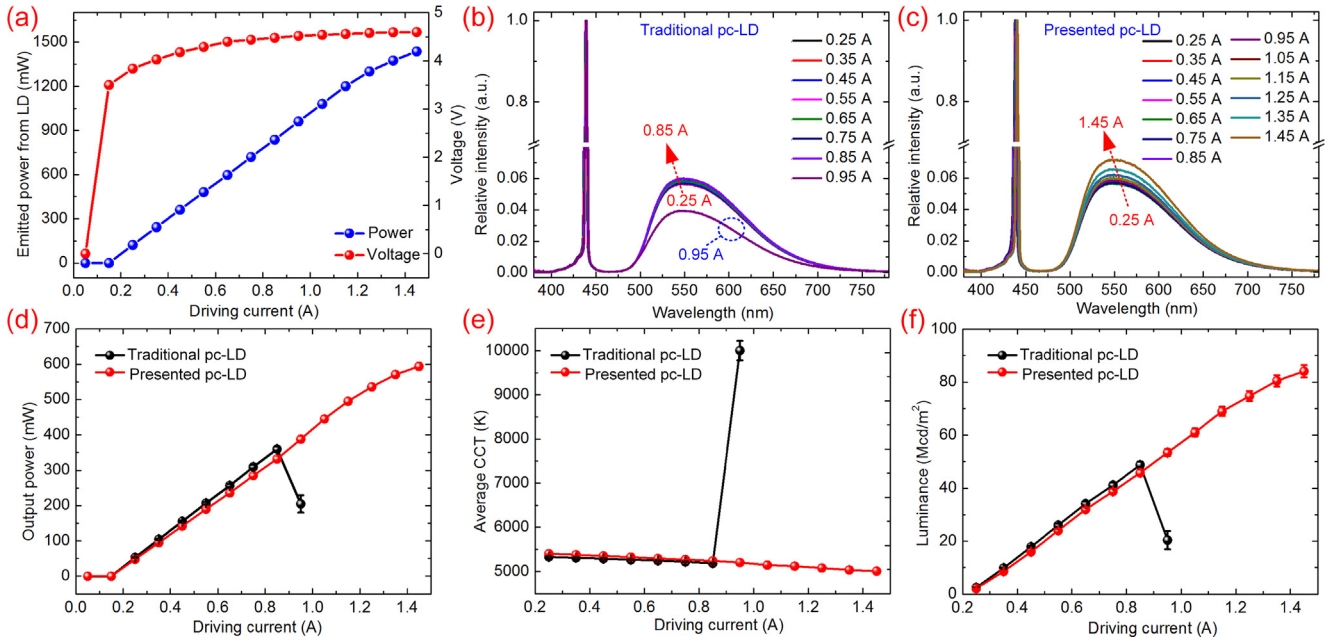

Fig. 10. (a) The measured P-V-I curves of LD. The relative spectral power distribution versus varying driving currents of the (b) traditional and (c) presented pc-LD. The comparisons of (d) output power, (e) average CCT, and (f) luminance between them versus varying driving currents.

the current rises from 0.85 A to 0.95 A, in which case the light conversion efficiency is very weak and the ratio of the blue light to yellow light is very large. In contrast, the CCT remains stable even when the current rises to 1.45 A for the presented type, which is due to the reduced phosphor temperature. It should be pointed out that the experimental proof-of-concept is not meant to be a comprehensive validation of the calculated results because not all the experimental conditions fully match the model, such as

the imperfect fabricated phosphor surface, phosphor parameters (absorption and scattering coefficients), non-collimated incidence, and so on. Despite these limitations, the experimental results verify the developing trends of the calculated results and also the effectiveness of double-sided phosphor cooling scheme in enhancing the opto-thermal performances of reflective pc-LD. It should also be noted that the geometrical feature of the sapphire substrate, i.e. thickness, plays a crucial role on heat transfer. When the thickness rises, the heat transfer area increases, contributing to a decrease of the phosphor temperature. In addition, the increase of the thickness may reduce the heat generation of the phosphor to a certain extent by reducing the incident optical power for the phosphor layer. However, the output optical power and luminance from the pc-LD may be also reduced with the increasing thickness. Therefore, there may be a complicated trade-off between the low phosphor temperature and high output power. In our future work, we will further study the effect of the thickness to find an optimum value according to the actual optical and thermal requirements.

5. Conclusions

In this work, a double-sided phosphor cooling scheme was presented by stacking a sapphire substrate on the phosphor layer to enhance the opto-thermal performances of the reflective pc-LD. Based on the opto-thermal model, it was found that both the maximum heat generation density and the maximum temperature were confined at the incident surface for the traditional reflective pc-LD. The maximum phosphor temperature was significantly reduced by adding another heat conducting path for the maximum heat confined in the incident surface through the sapphire substrate. Based on this point, the limiting excitation power against phosphor thermal quenching was enhanced by 165% under concentration of 0.05 g/cm^3 and spot radius of 2.5 mm. The experimental proof-of-concept was also conducted by fabricating and testing the presented reflective pc-LD. It was found that the sapphire substrate posed a marginal effect on the optical performance. More importantly, the presented scheme exhibited higher output power, luminance, and color stability under high excitation power. Therefore, the double-sided phosphor cooling scheme provides a simple but effective method to improve the overall opto-thermal performances of the reflective pc-LD, especially for high-power and high-luminance white illumination. In addition, a further enhancement is expected by combing this scheme with heat-conducting phosphors.

Declaration of Competing Interest

There are no conflicts of interest.

Acknowledgement

The authors would like to acknowledge the financial support by National Natural Science Foundation of China (51625601, 51576078, and 51606074), the Ministry of Science and Technology of the Peoplés Republic of China (2017YFE0100600), the financial support from Creative Research Groups Funding of Hubei Province (2018CFA001).

Appendix A. Supplementary material

Supplementary data to this article can be found online at https://doi.org/10.1016/j.ijheatmasstransfer.2019.118600.

References

[1] J.J. Wierer, J.Y. Tsao, D.S. Sizov, Comparison between blue lasers and light-emitting diodes for future solid-state lighting, Laser Photon. Rev. 7 (6) (2013) 963–993.
[2] X.B. Luo, R. Hu, S. Liu, K. Wang, Heat and fluid flow in high-power LED packaging and applications, Prog. Energy. Combus. Sci. 56 (2016) 1–32.
[3] Y.P. Ma, X.B. Luo, Packaging for laser-based white lighting: status and perspectives, J. Electron. Packag. (2019), https://doi.org/10.1115/1.4044359.
[4] X.B. Luo, X. Fu, F. Chen, H. Zheng, Phosphor self-heating in phosphor converted light emitting diode packaging, Int. J. Heat Mass Transf. 58 (2013) 276–281.
[5] J.J. Wierer, J.Y. Tsao, D.S. Sizov, The potential of III-nitride laser diodes for solid-state lighting, Phys. Status Solidi C 11 (3–4) (2014) 674–677.
[6] M. Cantore, N. Pfaff, R.M. Farrell, J.S. Speck, S. Nakamura, S.P. DenBaars, High luminous flux from single crystal phosphor-converted laser-based white lighting system, Opt. Express 24 (2) (2015) A215.
[7] A.F. George, S. Al-Waisawy, J.T. Wright, W.M. Jadwisienczak, F. Rahman, Laser-driven phosphor-converted white light source for solid-state illumination, Appl. Opt. 55 (8) (2016) 1899–1905.
[8] S. Masui, T. Yamamoto, S. Nagahama, A white light source excited by laser diodes, Electron. Commun. Japan 98 (5) (2015) 23–27.
[9] Y.P. Ma, X.B. Luo, Small-divergent-angle uniform illumination with enhanced luminance of transmissive phosphor-converted white laser diode by secondary optics design, Opt. Laser Eng. 122 (2019) 14–22.
[10] A. Lenef, J. Kelso, M. Tchoul, O. Mehl, J. Sorg, Y. Zheng, Laser-activated remote phosphor conversion with ceramic phosphors, Proc. SPIE 9190 (2014) 91900C.
[11] D.H. Lee, J. Joo, S. Lee, Modeling of reflection-type laser-driven white lighting considering phosphor particles and surface topography, Opt. Expr. 23 (15) (2015) 18872–18887.
[12] A. Lenef, J. Kelso, Y. Zheng, M. Tchoul, Radiance limits of ceramic phosphors under high excitation fluxes, Proc. SPIE 8841 (2013) 884107–884120.
[13] Y.P. Ma, W. Lan, B. Xie, R. Hu, X.B. Luo, An optical-thermal model for laser-excited remote phosphor with thermal quenching, Int. J. Heat Mass Transf. 116 (2018) 694–702.
[14] Y. Peng, Y. Mou, H. Wang, Y. Zhuo, H. Li, M.X. Chen, X.B. Luo, Stable and efficient all-inorganic color converter based on phosphor in tellurite glass for next-generation laser-excited white lighting, J. Eur. Ceram. Soc. 38 (16) (2018) 5525–5532.
[15] S. Li, Q. Zhu, D. Tang, X. Liu, G. Ouyang, L. Cao, N. Hirosaki, T. Nishimura, Z. Huang, R. Xie, Al_2O_3-YAG: Ce composite phosphor ceramic: a thermally robust and efficient color converter for solid state laser lighting, J. Mater. Chem. C 4 (37) (2016) 8648–8654.
[16] T.W. Kang, K.W. Park, J.H. Ryu, S.G. Lim, Y.M. Yu, J.S. Kim, Strong thermal stability of $Lu_3Al_5O_{12}:Ce^{3+}$ single crystal phosphor for laser lighting, J. Lumin. 191 (2017) 3–7.
[17] A. Correia, P. Hanselaer, Y. Meuret, Improving the opto-thermal performance of transmissive laser-based white light sources through beam shaping, Opt. Expr. 27 (8) (2019) A235–A244.
[18] P. Zheng, S.X. Li, L. Wang, T.L. Zhou, S.H. You, T. Takeda, N. Hirosaki, R.J. Xie, Unique color converter architecture enabling phosphor-in-glass (PiG) films suitable for high-power and high-luminance laser-driven white lighting, ACS Appl. Mater. Inter. 10 (2018) 14930–14940.
[19] Y. Peng, Y. Mou, Q.L. Sun, H. Cheng, M.X. Chen, X.B. Luo, Facile fabrication of heat-conducting phosphor-in-glass with dual-sapphire plates for laser-driven white lighting, J. Alloy. Compd. 790 (2019) 744–749.
[20] N. Abu-Ageel, D. Aslam, S. Member, Laser-driven visible solid-state light source for etendue-limited applications, J. Disp. Technol. 10 (8) (2014) 700–703.
[21] Y.P. Chang, J.K. Chang, W.C. Cheng, Y.Y. Kuo, C.N. Liu, L.Y. Chen, W.H. Cheng, New scheme of a highly-reliable glass-based color wheel for next-generation laser light engine, Opt. Mater. Expr. 7 (3) (2017) 1029–1034.
[22] X.R. Ding, M. Li, Z.T. Li, Y. Tang, Y.X. Xie, X.T. Tang, T. Fu, Thermal and optical investigations of a laser-driven phosphor converter coated on a heat pipe, Appl. Therm. Eng. 148 (2019) 1099–1106.
[23] J. Park, J. Kim, H. Kwon, Phosphor-aluminum composite for energy recycling with high-power white lighting, Adv. Opt. Mater. 5 (2017) 1700347.
[24] Y.P. Ma, R. Hu, X.J. Yu, W.C. Shu, X.B. Luo, A modified bidirectional thermal resistance model for junction and phosphor temperature estimation in phosphor-converted light-emitting diodes, Int. J. Heat Mass Transf. 106 (2017) 1–6.
[25] Y.P. Ma, M. Wang, J. Sun, R. Hu, X.B. Luo, Phosphor modeling based on fluorescent radiative transfer equation, Opt. Expr. 26 (13) (2018) 16442–16455.
[26] B.F. Shang, Y.P. Ma, R. Hu, C. Yuan, J.Y. Hu, X.B. Luo, Passive thermal management system for downhole electronics in harsh thermal environments, Appl. Therm. Eng. 118 (2017) 593–599.
[27] Y.P. Ma, X.B. Luo, Two-dimensional axisymmetric opto-thermal phosphor modeling based on fluorescent radiative transfer equation, J. Lumin. 214 (2019) 116589.
[28] J.M. Zhao, L.H. Liu, Discontinuous spectral element method for solving radiative heat transfer in multidimensional semitransparent media, J. Quant. Spectrosc. RA. 107 (1) (2007) 1–16.

[29] Z.Y. Liu, S. Liu, K. Wang, X.B. Luo, Measurement and numerical studies of optical properties of YAG: Ce phosphor for white light-emitting diode packaging, Appl. Opt. 49 (2) (2010) 247–257.
[30] L.J. Lyu, D.S. Hamilton, Radiative and nonradiative relaxation measurements in Ce^{3+} doped crystals, J. Lumin. 48 (1991) 251–254.
[31] H. Zheng, Y.M. Wang, L. Li, X. Fu, Y. Zou, X.B. Luo, Dip-transfer phosphor coating on designed substrate structure for high angular color uniformity of white light emitting diodes with conventional chips, Opt. Expr. 21 (2013) 933–941.